Earthquake Engineering, Tenth World Conference © 1992 Balkema, Rotterdam. ISBN 90 5410 060 5

Collapse simulation of steel frames with local buckling

K.Takanashi, K.-i.Ohi & Y.Chen
Institute of Industrial Science, University of Tokyo, Japan

L.Meng
Technical Research Institute, Fujita Corporation, Yokohama, Japan

ABSTRACT: An inelastic portion of steel beam–column is modeled as an assembly of spring elements, and a simple hysteresis rule is proposed to simulate their inelastic behaviors in consideration of the resistance deterioration due to local buckling. After the model parameters are chosen so that they match with the monotonic test results, the validity of the model when it is used in the response analysis is checked through the comparison with the results of the on–line response tests, some of which simulate the complete collapse of steel frames.

1 INTRODUCTION

To establish the ultimate safety of frames to earthquake loading, it is indispensable to carry out a number of response simulation over various structural parameters to an extensive set of earthquake motions. Constitutive modeling used for such simulation is better to be as simple as possible, but should never neglect essential properties of inelastic structural behaviors. Especially for steel frames, several inelastic behaviors, such as yielding, strain–hardening, Bauschinger's effect, local buckling, P–Δ effect, and so on, should be appropriately considered in the model construction.

In this paper, an analytical model termed "multi-spring inelastic joint" (Ohi, 1992) is studied to simulate the behaviors of inelastic portions of steel beam-columns subject to uni–axial bending and axial load. Similar modeling was already proposed for concrete members subject to bi–axial bending (Lay, 1984). A simple hysteresis rule suitable to express the abovementioned inelastic behaviors is also proposed herein. After model parameters are calibrated to the results of the monotonic loading tests, the validity of the model when it is used in the response analysis is demonstrated through the comparison with the results of the on-line pseudo–dynamic tests, which are performed on H–shaped and square box specimens.

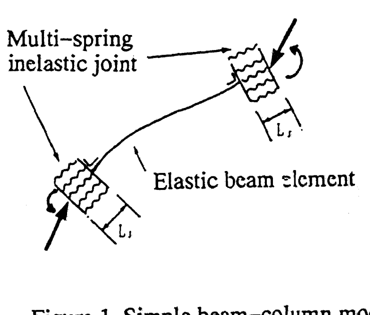

Figure 1 Simple beam–column model

2 A SIMPLIFIED BEAM–COLUMN MODEL

A steel beam–column is regarded as an assembly of two kinds of elements as shown in Figure 1: one is an elastic beam, and the other is an inelastic joint. In the following analysis, nodes are located at the tips of these two elements, and geometrical non–linearity or P–Δ effect is considered only for the displacements of these nodes by updating each element coordinate system in the incremental analysis.

The inelastic joint consists of four axial springs and a shear panel as shown in Figure 2. In the presence of the stress transmission among the springs and the panel, each spring may carry axial force varying along the joint axis, but the axial force at the center is chosen as the representative axial force of each spring.

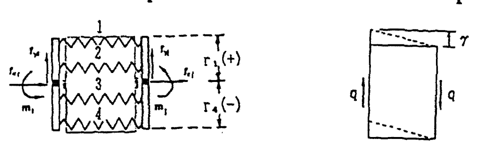

(a) Axial springs (b) Shear panel

Figure 2 Multi–spring inelastic joint

2.1 Hysteresis model for springs

Two different skeleton curves are used for the tension-side and the compression–side behaviors of each spring, respectively. The tension–side skeleton curve shall be arranged similar to the uni–axial stress–strain curve of steel material, and the compression–side skeleton curve shall be arranged in consideration of the strength deterioration due to local buckling. Piecewise linear models are adopted herein for the both side skeleton curves as shown in Figure 3(a).

Two imaginary points termed 'target points' on the skeleton curves, one for each side, are considered herein. These points are referred to determine unloading and reloading paths. Each target point is set at the elastic–limit point in the initial state. When a loading beyond the elastic-limit is made along one side skeleton with a certain amount of plastic deformation, the target point of the loading side moves together with the loading point, and at the same time, the other side skeleton curve including the other target point shall be shifted to the loading direction as much as Ψ times the *plastic deformation.* Such a loading procedure on the skeleton curve is illustrated in Figure 3(b). If Ψ is set to zero, neither hardening nor degrading occurs during cyclic reversals within the past peak amplitudes. If Ψ is set to one, the hysteresis includes no softening due to the Bauschinger's effect. Actual behaviors of steel members are believed to fall on the intermediate state between these two extreme states.

Unloading and reloading paths are modeled as portions of the Ramberg–Osgood function, denoted by $\delta = R_{-O}(P)$. The parameters included in this function is determined to satisfy (i) $\delta_U = R_{-O}(P_U)$, where the point (δ_U, P_U) is the last unloading point, (ii) $\delta_T = R_{-O}(P_T)$, where the point (δ_T, P_T) is the target point on the skeleton curve in the unloading and reloading direction, and (iii) $K_1\, dR_{-O}/dP\,(P_U)=1$, where K_1 is the initial elastic stiffness. These conditions are illustrated in Figure 3(c). The tangent stiffness denoted by $K^*(=dP/d\delta)$ is derived from these conditions as:

$$K^* = K_1 K_a / [\, K_a + (K_1-K_a)|(P-P_U)/(P_T-P_U)|^{r-1}]$$

where $K_a = (P_T-P_U)/(\delta_T-\delta_U)$

2.2 Calibration of model parameters with monotonic test results

Monotonic bending tests were carried out on welded H-shaped and square box beam-columns under constant axial loads as shown in Figure 4. H-shaped and square box sections with various *width-thickness* ratios were welded from steel plates in the same lot: the width-thickness ratios for half the flange width of H-shaped section are 6, 8, and 10, and those for the full nominal width of square box section are 20, 30, and 40. The cases of no axial load and the constant axial load with 40 or 20 percent of the yield axial load were considered.

The yield stress and the maximum tensile strength needed to arrange the tension-side skeleton curve are derived from the preliminary tension test results: 450 MPa and 590 MPa in average, respectively. As for the compression-side skeleton curve, it is empirically recognized that the maximum moment capacity of the beam-column would be underestimated if the results of the stub column compression tests were used as they were. This might be resulted from the difference of the stress gradient in the beam-column tests and the stub column tests. Consequently, other parameters than Young's modulus, the yield stress, the tensile strength, and the length of the inelastic joint, assumed equal to the column depth, are adjusted by trial and errors so that the simulated monotonic curves totally match with the corresponding test curves.

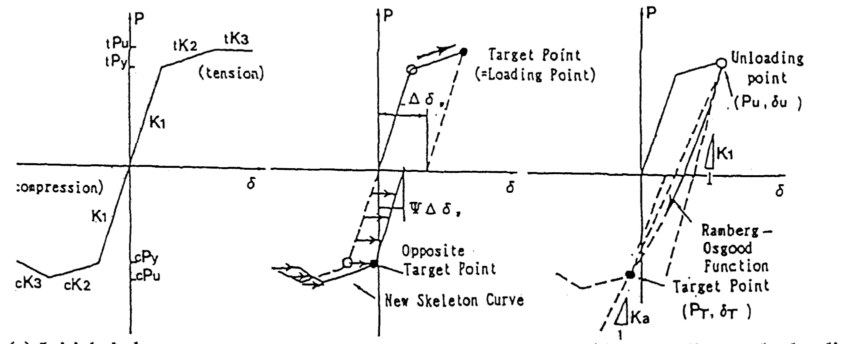

(a) Initial skeleton curves (b) Shift of skeleton curve (c) Unloading and reloading

Figure 3 Hysteresis rule for axial springs

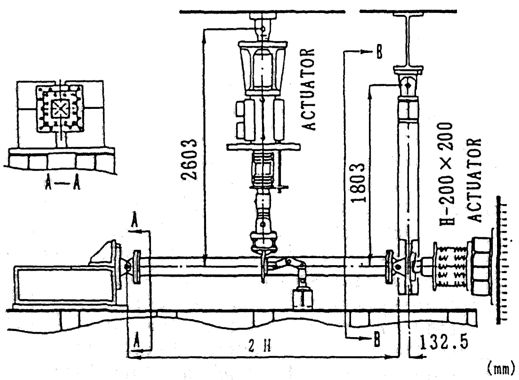

Figure 4 Test setup

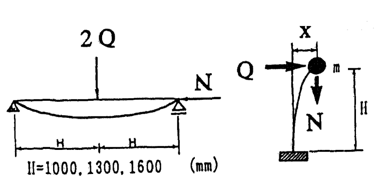

(a) Loading test

(b) Vibrational system analyzed in on-line tests

Figure 5 Test schema

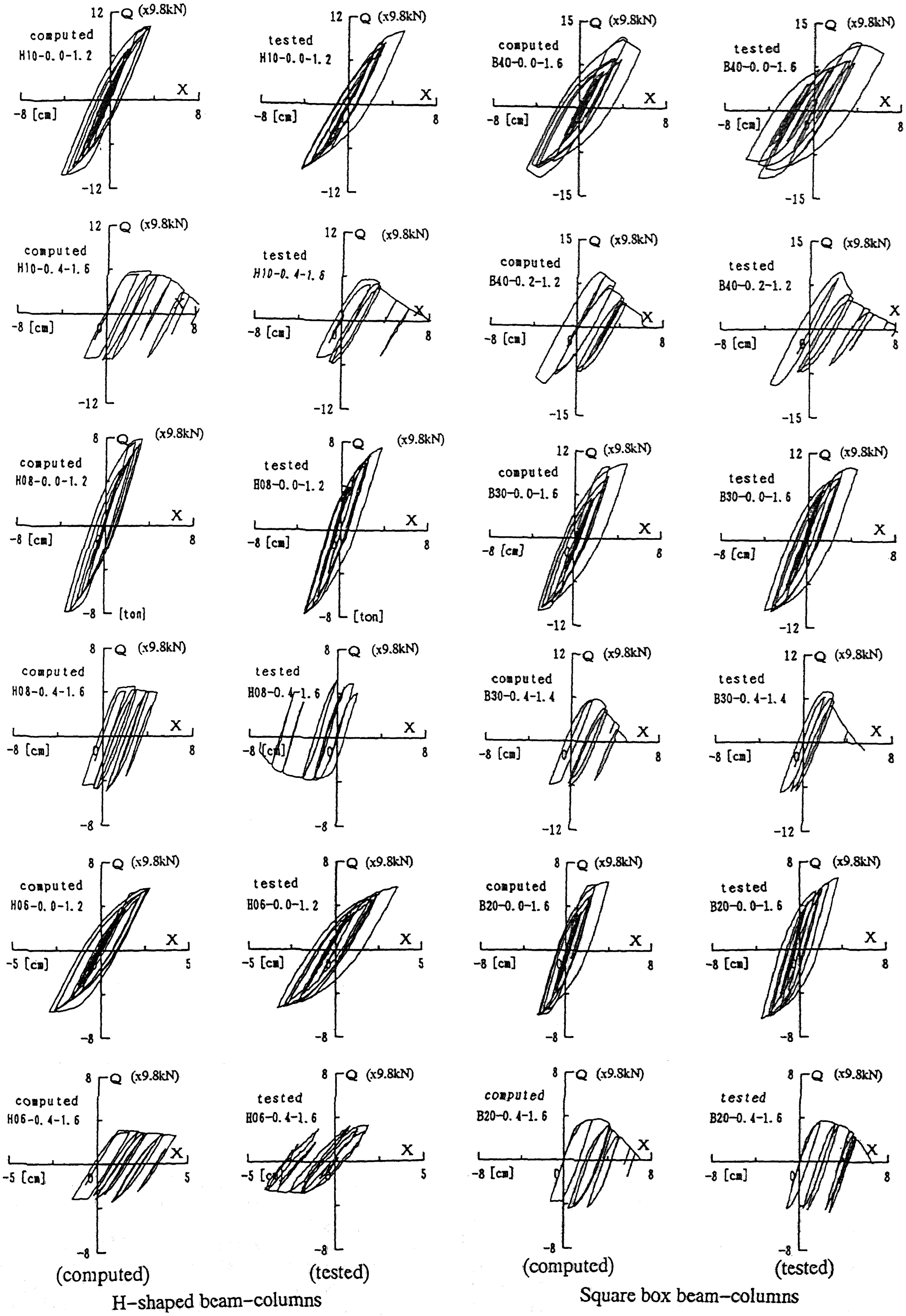

Figure 6 Hysteresis loops under earthquake loading —— tested and computed (parameters: Ψ =0.8, r =5)

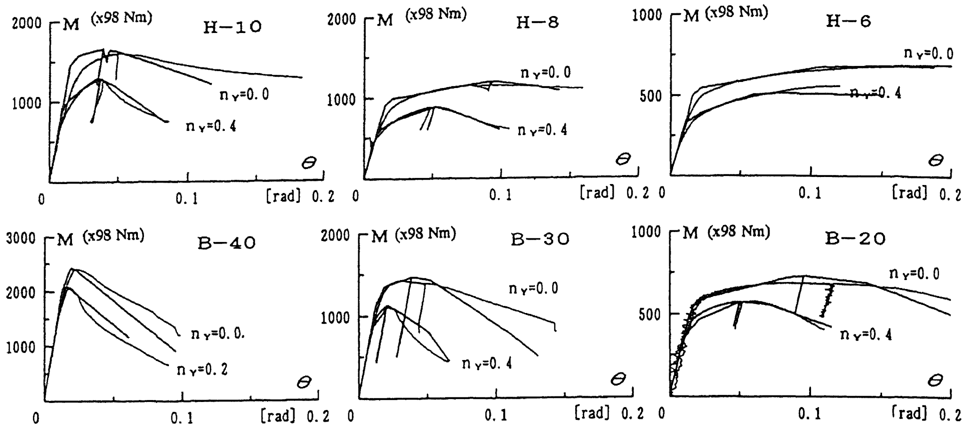

Figure 7 End moment vs. rotation under monotonic loading ———— tested and modeled

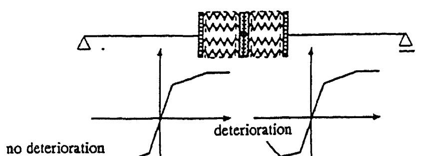

Figure 8 Analyzed beam-column

In the loading tests, the yielding and the initiation of the local buckling were detected at the both sides of the central loading point, but after that, the local buckling failures were brought up larger at only one side. Considering this observation, two inelastic joints are inserted at the center of the beam-column and no resistance deterioration is assumed for one of the inelastic joints in the following analyses, as shown in Figure 8. The load-deflection curves observed in the monotonic loading tests and those simulated by the models are shown in Figure 7.

3 COMPARISON WITH ON-LINE TEST RESULTS

On-line response tests under earthquake loading were performed by use of the same test setup used in the monotonic loading tests described in Section 2.2. The N-S component of El Centro 1940 was used as the input ground motion, the intensity of which was adjusted to attain two kinds of damage levels for each cases: one is moderate yielding for the case of no axial load, and the other is nearly in the complete collapse state for the case of constant axial load. In these tests, half of the load applied at the center of the specimen during the tests was regarded as the restoring force of the single-degree-of-freedom vibrational system shown in Figure 5. It should be noted that the deterioration of the lateral resistance of the vibrational system is induced by not only local buckling failure but also the P-Δ effect due to the constant axial load applied. Fictitious mass was arranged from the elastic stiffness measured prior to the on-line tests so that the natural period would be commonly 0.8 seconds, and no fictitious viscous damping effect was assumed.

Numerical simulations were carried out based on the multi-spring joint models arranged in Section 2.2. Hysteresis loops observed in the on-line tests and the numerical simulations are compared in Figure 6. The numerical simulation does not always agree exactly with the displacement history observed in the on-line test, that is, the simulated direction in which major permanent set occurs is sometimes opposite to the test result. Even in such a case, however, no fatal errors are recognized in the prediction of the global damage level and the peak response displacement.

4 CONCLUDING REMARKS

Inelastic portions of steel beam-columns are modeled as an assembly composed of inelastic springs and a shear panel. Also, a hysteresis rule suitable for the spring elements in such a modeling is proposed in consideration of strain-hardening, softening due to the Bauschinger's effect, and resistance deterioration due to local buckling failure as well.

After the model parameters were calibrated to the results of the monotonic loading tests which were performed on H-shaped and square box beam-columns with various width-thickness ratios, response analyses based on the inelastic joint model were carried out and compared with the results of the on-line response tests under earthquake loading.

It is demonstrated that the global responses are well predicted for the practical purpose by the present model even in such a final collapse state as the lateral resistance of the frame almost disappears.

REFERENCES

Lai, S.S., G.T. Will & S. Otani 1984. Model for inelastic bi-axial bending of concrete members, ASCE, Vol.110, ST11.

Ohi, K. & K. Takanashi 1992. Multi-spring joint model for inelastic behaviors of steel members with local buckling, In Y. Fukumoto & G. Lee (eds.), Stability and ductility of steel structures under cyclic loading, CRC Press: 215-224.